Tu A2 12

Imaging of Multiples and its Application on Single Sensor Data

J. Mao (TGS), S.N. Baldock* (TGS), J. Sheng (TGS)

Summary

It is recognised that multiple reflections contain valuable information not present in primary reflections. Multiple energy reflects from a larger spatial area than the corresponding primaries for the same reflector. For a given common reflection point (CMP) multiples contain a smaller set of reflection angles than the primary reflection. These facts make multiple reflections of interest for improving the quality of images at shallow depths when the water depth is shallow and/or the recording geometry is somewhat coarse. Several methodologies exist for imaging multiples. Wavefield separation techniques are widely used to image upgoing and downgoing wavefields separately. We describe a new approach for wavefield separation on single sensor data. The image is formed from the receiver ghost (downgoing wavefield) and deghosted data (upgoing wavefield). Application to a wide azimuth dataset demonstrates the benefits and potential pitfalls of the approach.

Introduction

The last few years have seen a shift away from the view that multiple reflections are noise that must be removed prior to imaging. Multiple reflections contain information useful for improving the results of subsurface imaging. This is particularly the case for surveys located in shallow water and for recording geometries that are somewhat sparse in their receiver sail line spacing. The advantages of using multiples in imaging are increased subsurface coverage and increased subsurface illumination (Figure 1).

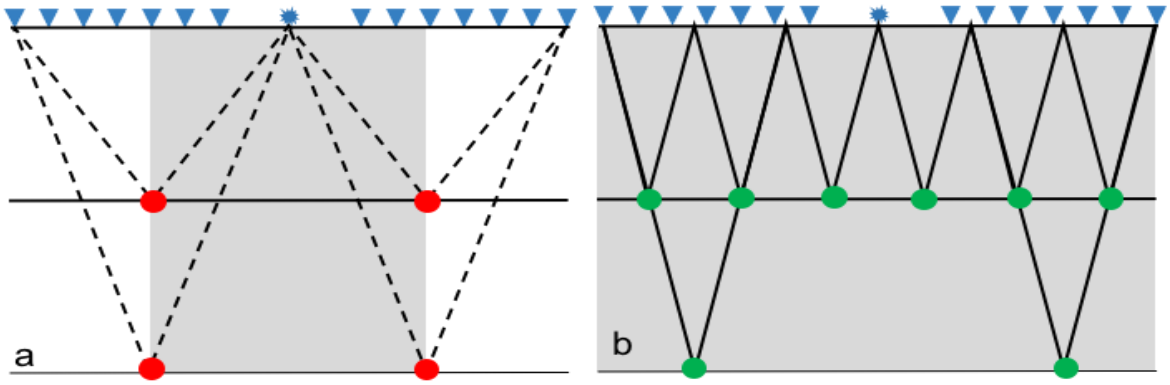

***Figure 1**. The benefits of using multiples in imaging are increased subsurface coverage and increased subsurface illumination.*

Many solutions to imaging with multiples combine an areal source with a deconvolution imaging condition in a one-way or two-way imaging scheme. The areal source is formed by using part of the total wavefield recorded at the receivers as the source term. This improves illumination and coverage by significantly increasing the shot density: the shot density becomes equal to the receiver density.

To successfully utilize multiple energy some challenges must be overcome, the most significant being that of crosstalk between different orders of multiples. Crosstalk is created by a correlation between energy in the source and receiver wavefields that does not have a reflection point at the depth at which the imaging condition is applied. A deconvolution imaging condition is critical to reduce crosstalk noise.

In general imaging with multiples using wave equation methods takes one of two approaches. One approach images primaries and multiples separately. In this case, the correct image is formed by the sum of crosscorrelations between primaries and first-order multiples, and between multiples crosscorrelated with multiples of one order higher. If we consider primaries as a multiple of order i=0, crosstalk will occur for crosscorrelations between multiples of order i and multiples of all other orders except for $i \neq i+1$.

This is illustrated in Figure 2, where the 2D SIGSBEE synthetic model has been migrated using primaries and multiples. The yellow arrows indicate places where crosstalk events can be seen to cut across the true events. The crosstalk events appear deeper than the true reflections. One way to reduce crosstalk in the image is to control the orders of multiples that are imaged together in the migration (Liu et al., 2016).

Another approach is to separate the wavefield into upgoing and downgoing components. This is a solution that avoids the need to separate out orders of multiples while reducing the excessive crosstalk that will occur if both primaries and multiples are imaged together. The downgoing wavefield is propagated forward in time and the upgoing wavefield is propagated backward in time. In this case the true image is given by the crosscorrelation of a downgoing multiple with an upgoing multiple of one order higher. Both source and receiver wavefields contain multiples of all orders and so crosstalk will occur at depths both earlier and later than the true reflection (Lu et al., 2016).

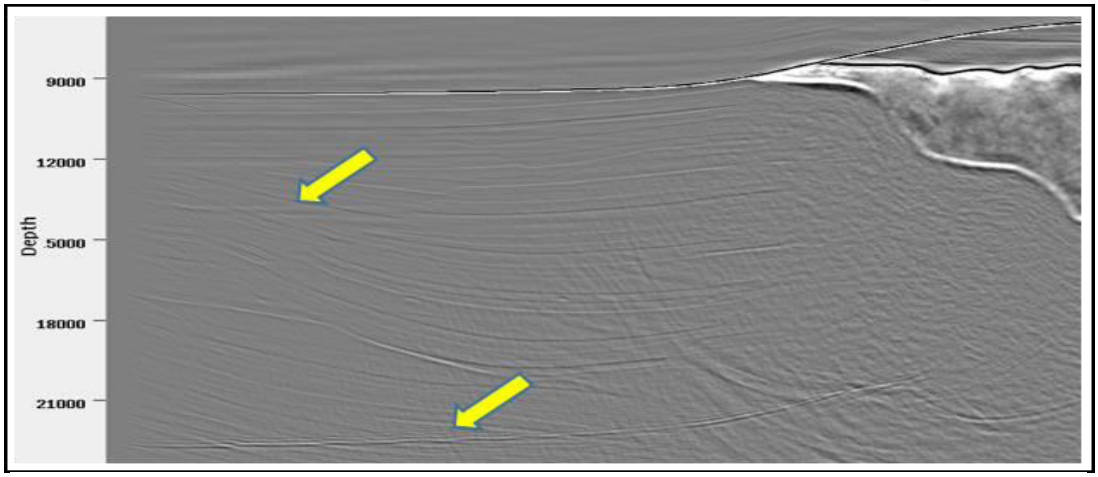

Figure 2 *Migration of the SEG salt model using primaries and multiples. The crosstalk events appearing deeper than the true image are indicated by the yellow arrows.*

Wavefield separation can be achieved using multicomponent receivers recording pressure and velocity and good results have been achieved with this method (Lu et al., 2015). However, the need for dual sensor acquisition limits the range of data sets to which the technique can be applied. In the next section we show that wavefields can be separated effectively for single sensor data by careful separation of the receiver ghost energy from the total recorded wavefield.

Methodology

The receiver on a towed streamer simultaneously records upgoing and downgoing energy. The downgoing wavefield is a delayed copy of the upgoing wavefield scaled by the reflection coefficient at the sea surface:

$$W = U + D$$
$$= U(1 + re^{i\omega z}). \qquad (1)$$

Here r is the reflection coefficient at the sea surface and z is the receiver depth. W, U and D are the total, upgoing and downgoing wavefields respectively. The upgoing wavefield can be extracted by deghosting the recorded wavefield:

$$U = \frac{W}{1+re^{i\omega z}}. \qquad (2)$$

The downgoing wavefield is found by subtracting the upgoing wavefield from the total recorded wavefield. The upgoing (deghosted) and downgoing (receiver ghost) wavefields may then be input into a wave-equation migration as described in the previous section. Figure 4 illustrates our methodology: Figure 4a describes the process in flow chart form; Figure 4b illustrates the separation into upgoing and downgoing wavefields for some select ray paths.

In order to reduce crosstalk, a critical step is the use of a deconvolution imaging condition (equation 3) in place of the standard crosscorrelation imaging condition. While this will not remove coherent cross-talk, incoherent crosstalk is significantly reduced and the overall signal to noise greatly improved.

$$R(x) = \sum_{x_s} \sum_{\omega} \frac{P_{up}(x_s,x,\omega)P^*_{down}(x_s,x,\omega)}{\langle P_{down}(x_s,x,\omega)P^*_{down}(x_s,x,\omega)\rangle_x + \varepsilon(x_s,x,\omega)} \qquad (3)$$

Results

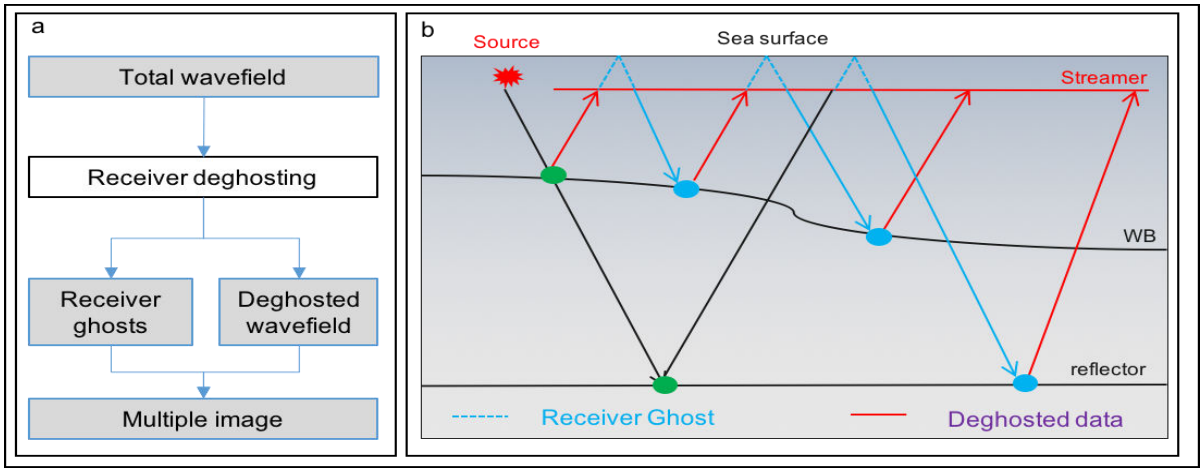

Figure 3 *a) a flow chart of the wavefield separation and imaging workflow; b) illustrates the different wavefields, the downgoing wavefield (blue) is composed of the receiver ghost, the upgoing wavefield (red) is composed of the deghosted data. Primary reflection points are shown in green and multiple reflation points in blue.*

Results are illustrated on a wide azimuth towed streamer data from the Gulf of Mexico. The sail lines are 600 m apart with an antiparallel shooting configuration. Wavefield separation was performed using a tau-*p* domain adaptive windowed deghosting approach (Zhang, 2016). Figure 5 shows the results on a depth slice at 800 m. The primary image (Figure 4a) is formed using a crosscorrelation imaging condition and a point source for the source term. The shot line spacing gives rise to a lack of

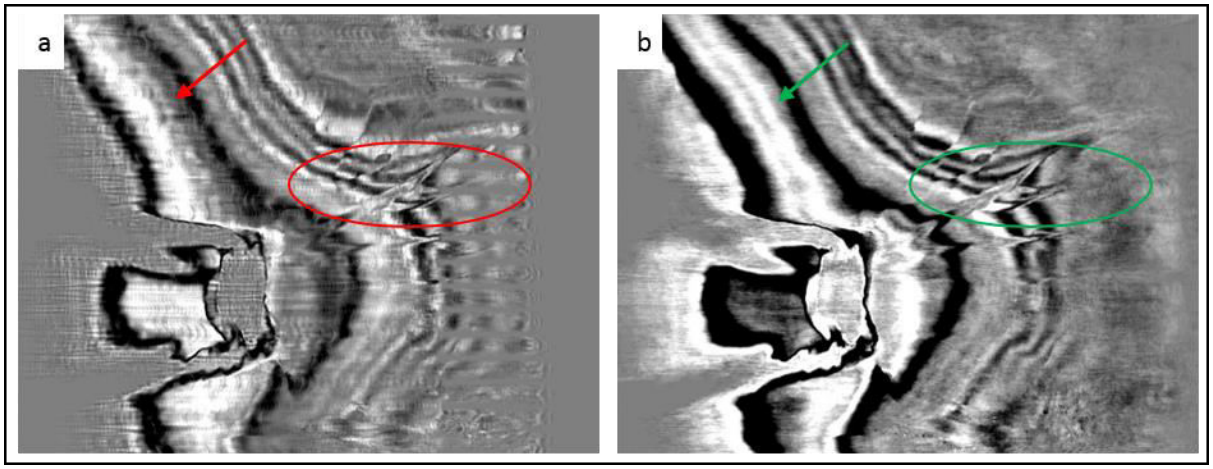

Figure 4 *Depth slice of wide azimuth towed streamer data at 800 m a) primary image; b) image using separated wavefields.*

near angle reflections at shallow depths creating a strong acquisition footprint and loss of resolution. Figure 4b shows the corresponding image formed by imaging the upgoing and downgoing wavefields. By considering each receiver as a source location the crossline shot spacing is reduced from the sail line spacing to the cable spacing. This increases illumination and near angle reflections, which, in turn removes the acquisition footprint and improves shallow resolution. Areas where this can be observed in Figure 4 are indicated by a circle and an arrow.

Figure 5 shows an inline and crossline from the same volume. The inline from the separated wavefield image (Figure 5b) clearly shows the increased coverage, which occurs on both ends of the line due to the antiparallel shooting configuration. The additional coverage allows better definition of the shallow salt body. The resolution of top and base of salt is also increased. The footprint seen on the depth

slice, is again clearly visible on the crossline (Figure 5c). Figure 5d, the result from imaging with separated wavefields, shows increased resolution and coverage in the shallow portion.

We note three factors that contribute to the success or failure of the method. *Shallow dip*: multiples from dipping reflectors may not be recorded by the receiver spread and so cannot contribute to the image. In Figure 5b the imaging of the dipping right-hand flank of the salt dome is less well imaged due to this. *Crosstalk*: creates artificial events and reduces resolution. In Figure 5d crosstalk has reduced the resolution of the deeper reflectors. *Deghosting*: in our method, the wavefield separation is only as good as the deghosting step. Therefore, careful preparation for, and QC of, the deghosting is critical.

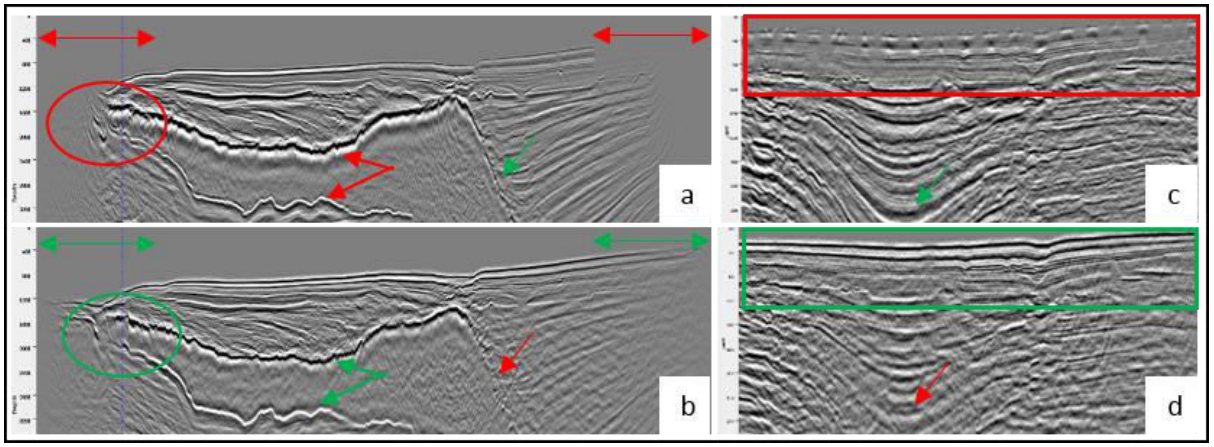

Figure 5 Inline and crossline: a) inline primary image; b) inline image using separated wavefields; c) crossline primary image; d) crossline image using separated wavefields.

Future work will focus on further reduction of crosstalk and the extension of the method from stack images to gathers.

Conclusion

The use of multiple reflections in imaging is able to improve shallow resolution and increase coverage. Imaging of multiples using separated wavefields has been successfully applied with good results in the case of dual sensor cables. We have presented a methodology for separating wavefields on data recorded with single sensor cables and demonstrated its effectiveness on a real data case. Potential pitfalls of the method and areas for future work were outlined.

Acknowledgements

We thank TGS for permission to publish the data. We also thank Zhiming Li, Bin Wang, and Xuening Ma for helpful discussions and ideas, Brad Beck for preprocessing the data and Connie VanSchuyver for proofreading the paper.

References

Lu S., Whitmore, D., Valenciano, V. and Chemingui, N. [2015] Separated-wavefield imaging using primary and multiple energy. The Leading Edge, 34, 770-778.

Lu S., Whitmore, N., Valenciano, V., Chemingui, N. and Ronholt, G. [2016] A practical crosstalk attenuation method for separated wavefield imaging. 86th Annual International Meeting, SEG, Expanded Abstracts, 4235-4239.

Liu Y., Liu, X., Osen, A., Shao, Y., Hu, H. and Zheng, Y. [2016] Least-squares Reverse Time Migration Using Controlled Order Multiples. 78th EAGE Conference, Expanded Abstracts, 1-5.

Zhang, Z., Wu, Z., Wang, B. and Ji, J. [2016] Adaptive Windowed Deghosting – Applications to FAZ Acquisition. 78th EAGE Conference, Expanded Abstracts, 1-5.